Large Scale Solid State Synthetic Technique for High Performance Thermoelectric Materials: Magnesium-Silicide-Stannide

Daniel C. Ramirez[†], *Leilane R. Macario*[†], *Xiaoyu Cheng*[†], *Michael Cino*[‡], *Daniel Walsh*[‡], *Yu-Chih Tseng*[‡], *Holger Kleinke*[,†]

[†] Department of Chemistry and Waterloo Institute for Nanotechnology, University of Waterloo, Waterloo, ON N2L 3G1, Canada

[‡]CanmetMATERIALS, Natural Resources of Canada, 183 Longwood Road South, Hamilton, Ontario L8P 0A5, Canada

Supporting Information

Hot-Pressing

The hot-press used is the FCT Ingenieurkeramik GmbH model HP W 400 SD/KD. The press uses an indirect hot pressing method where the heating occurs through the mold by convection. We have maximal heating capacity of 2200°C with 180 kW of heating power. The press has a 4000 kN pressing capacity, and the ultimate vacuum is 5.0 x 10^{-2} mbar. The molds are solid graphite – the powder to be compacted is separated from the graphite by a graphite foil about the perimeter, on top and bottom pressing surfaces.

Powder X-ray Diffraction

The diffractometer used was the INEL XRG 3000 Powder Diffractometer. Copper-Kα1 radiation was generated using 30 kV and 30 mA for electron bombardment onto a water cooled copper source. The x-rays were monochromated using a germanium single crystal to produce wavelength of 1.5406 Å. The powder sample is rotated when exposed to the x-rays and diffraction is detected using position sensitive arc detector.

Seebeck and Electrical Conductivity

The measurements were performed using ZEM-3 manufactured by ULVAC RIKO M8 type with maximum heating to 800ºC. Parallelepiped samples are positioned between two current electrodes with heating capabilities. Multifunctional voltage and temperature probes are contacted to a long face of the sample with pressure; probe distance measured via calibrated camera. The chamber is heated under helium atmosphere; at each temperature electrical conductivity is measured via the 4-probe method while Seebeck coefficient is measured via the static DC method.

Thermal Diffusivity

The thermal diffusivity was measured with the LFA457 from Netzsch, maximum temperature 1100°C. The measurements were in done in Ar environment. Square samples are positioned in a sample holder between a laser source (Nd:Glass 1054 nm) and liquid N_2 cooled InSb thermal detector. Thermal diffusivity accuracy is ± 3% over the entire range.

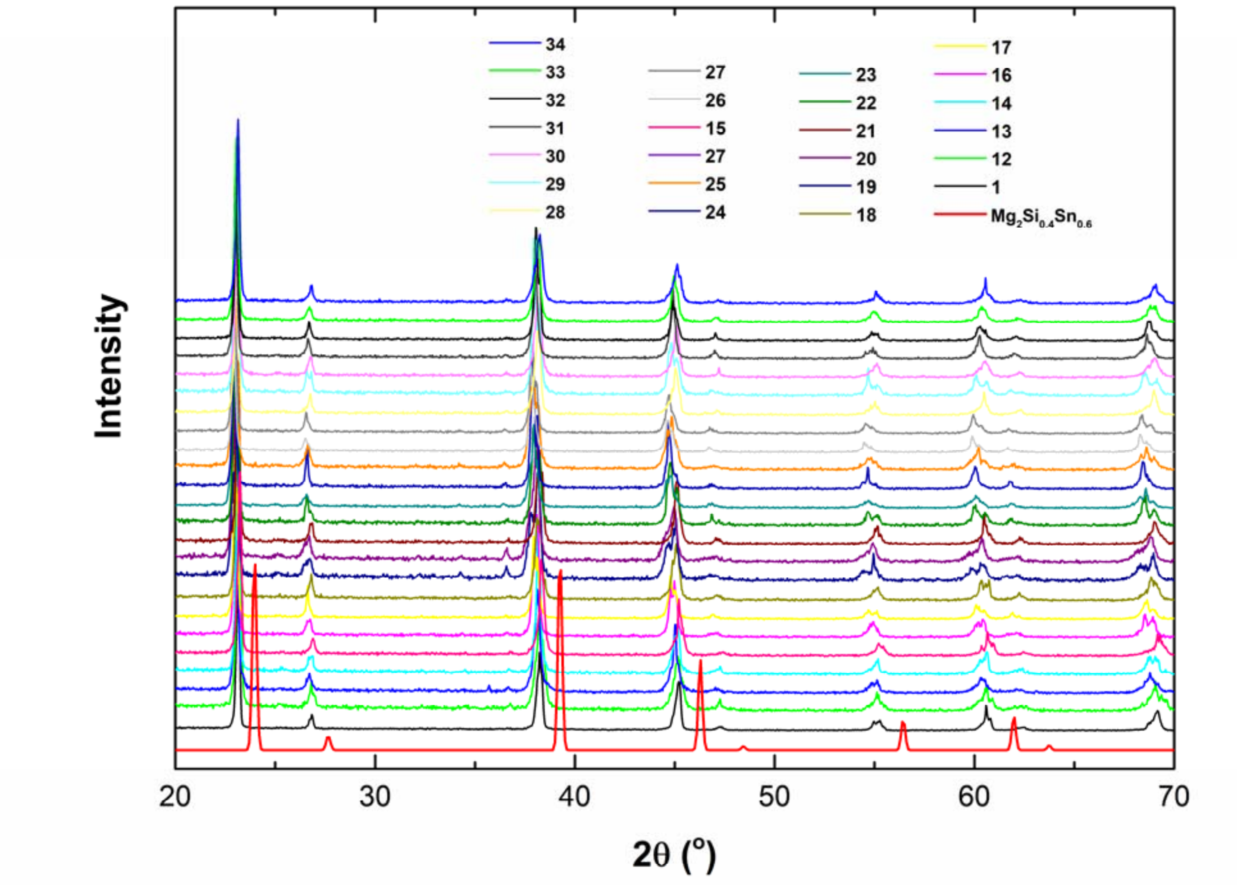

Figure S1. PXRD verifying quality of as synthesized ingots of $Mg_2Si_{0.3}Sn_{0.67}Bi_{0.03}$ by comparing to calculated $Mg_2Si_{0.4}Sn_{0.6}$ (red). The expected phase shift from the difference in solid solution stoichiometry is seen. The majority of samples display a small impurity peak at 2θ = 37º associated with the presence of elemental magnesium. Samples containing large amounts of magnesium (19, 20) or other impurities (13, 25) were omitted from further experiments. Samples were measured for 10 minutes.

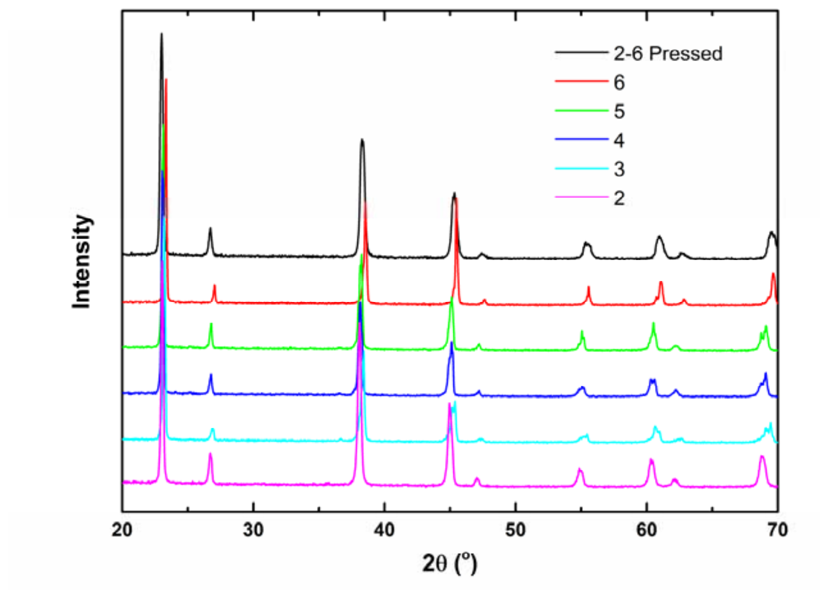

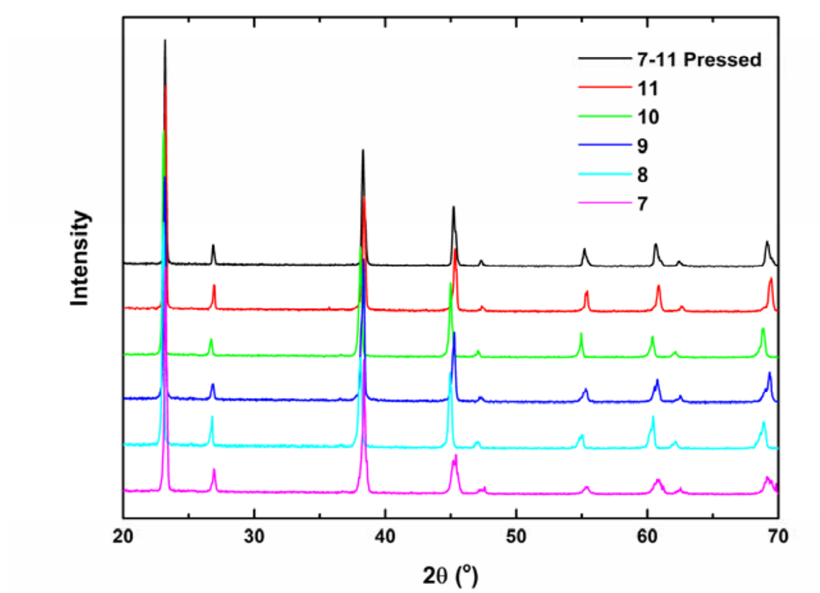

Figure S2: PXRD of as synthesized ingot samples (a) 2-6, (b) 7-11, and sintered pellets obtained from combined powders of $Mg_2Si_{0.3}Sn_{0.67}Bi_{0.03}$. The sintering results display complete miscibility of all samples indicated by singular peaks. Disappearance of the elemental magnesium peaks ($2\theta = 37^o$) in the pressed sample is observed. Samples were measured for 20 minutes.

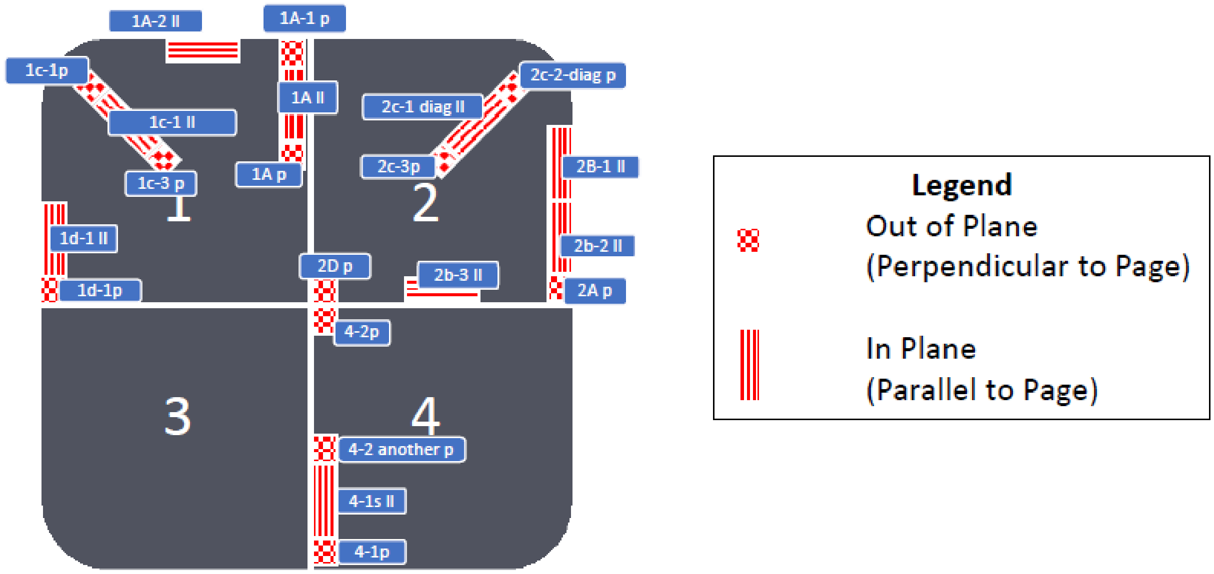

Figure S3. Machining diagram of the large pellet of $Mg_2Si_{0.3}Sn_{0.67}Bi_{0.03}$ with parallelepiped samples cut for Seebeck coefficient and electrical conductivity measurements as performed on ULVAC-RIKO ZEM-3 apparatus.

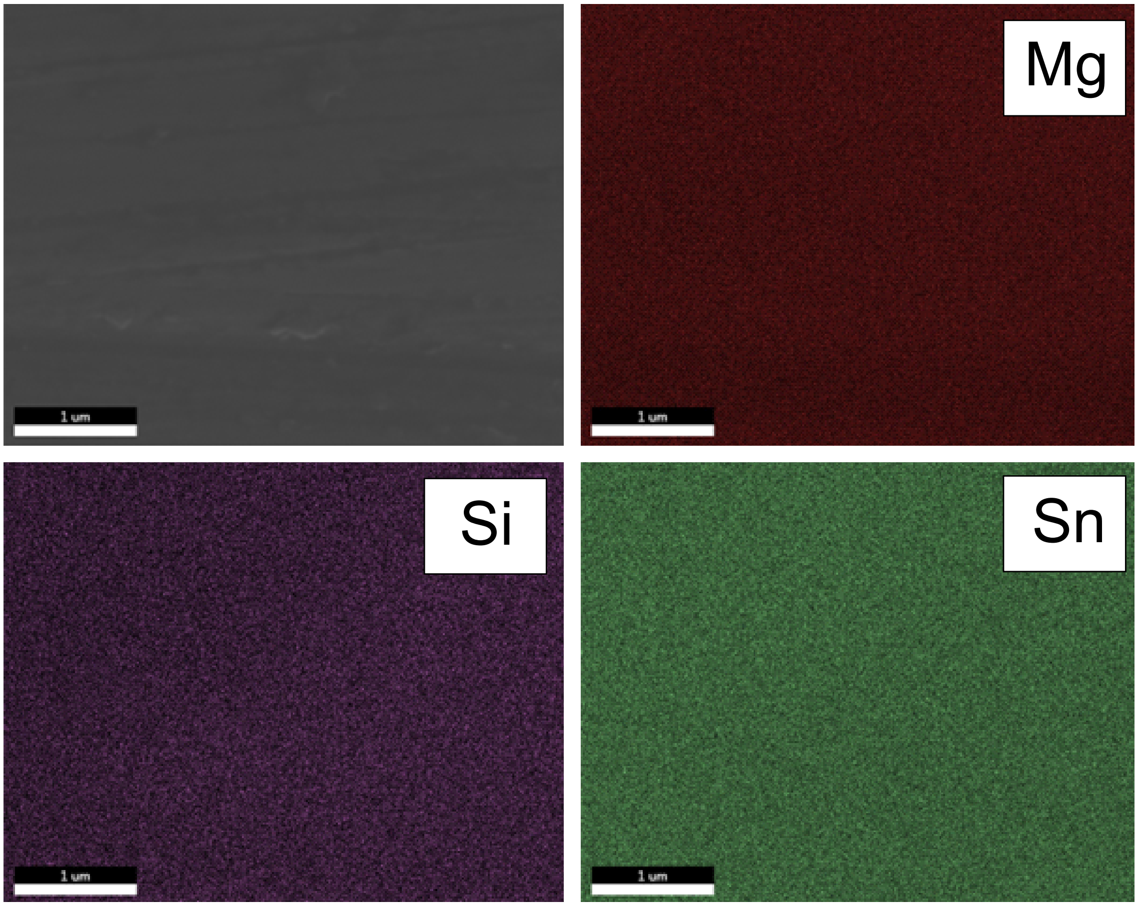

Figure S4. SEM pictures of a hot-pressed pellet of $Mg_2Si_{0.3}Sn_{0.67}Bi_{0.03}$ after the property measurements.

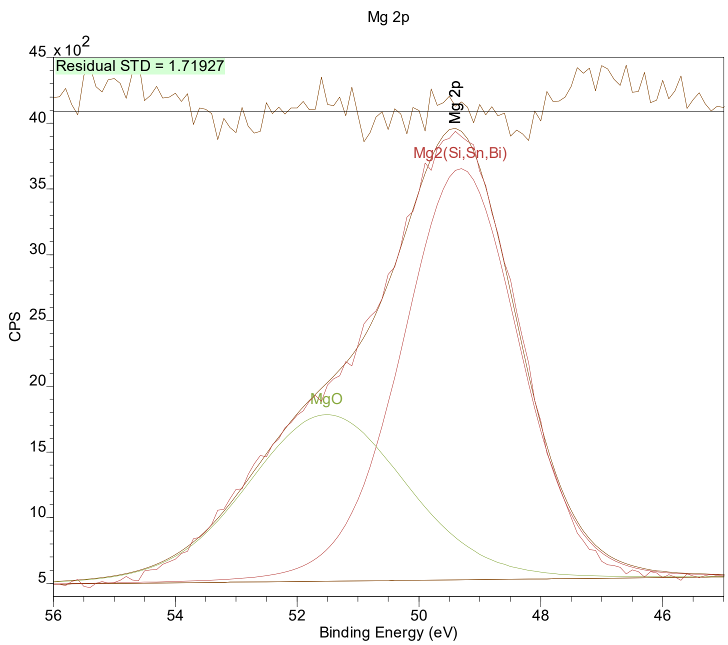

Figure S5. Mg 2*p* region of $Mg_2Si_{0.3}Sn_{0.67}Bi_{0.03}$.

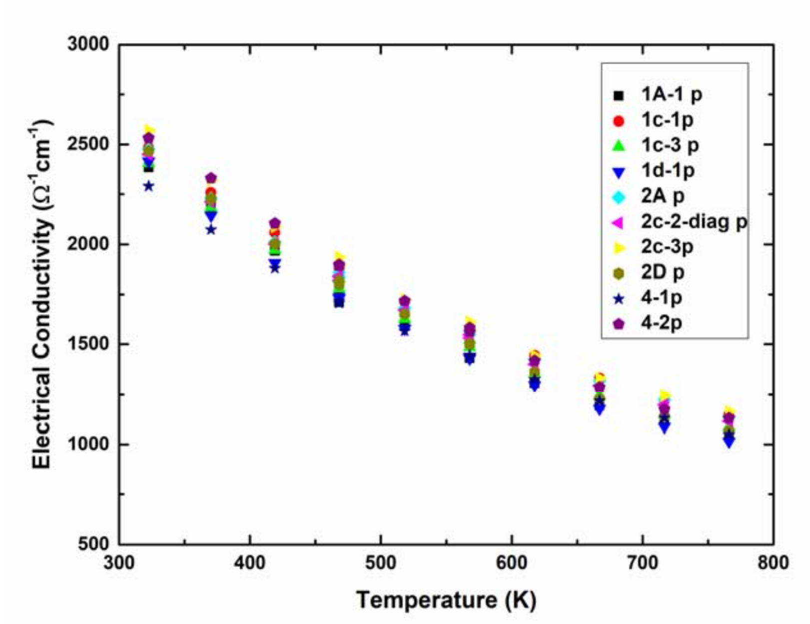

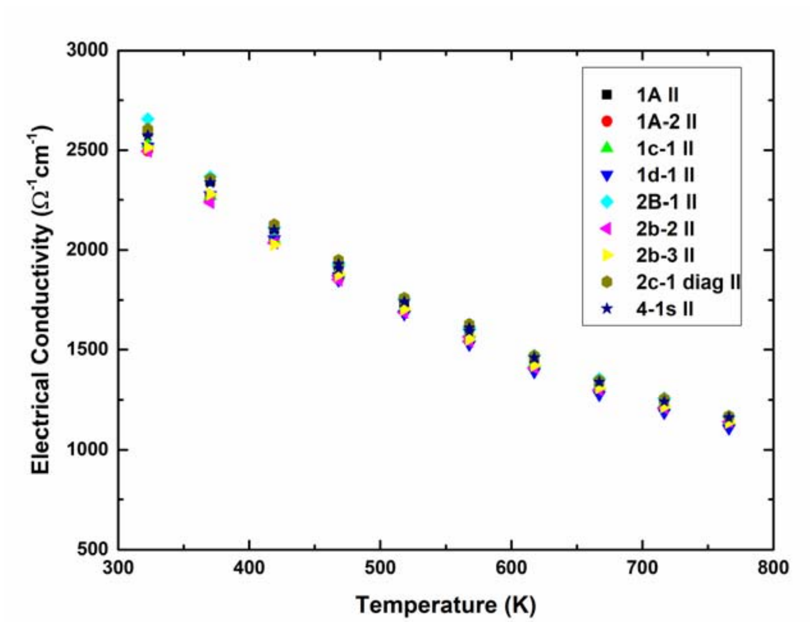

Figure S6. Electrical conductivity vs temperature measurements on machined samples obtained as shown in Figure S3.

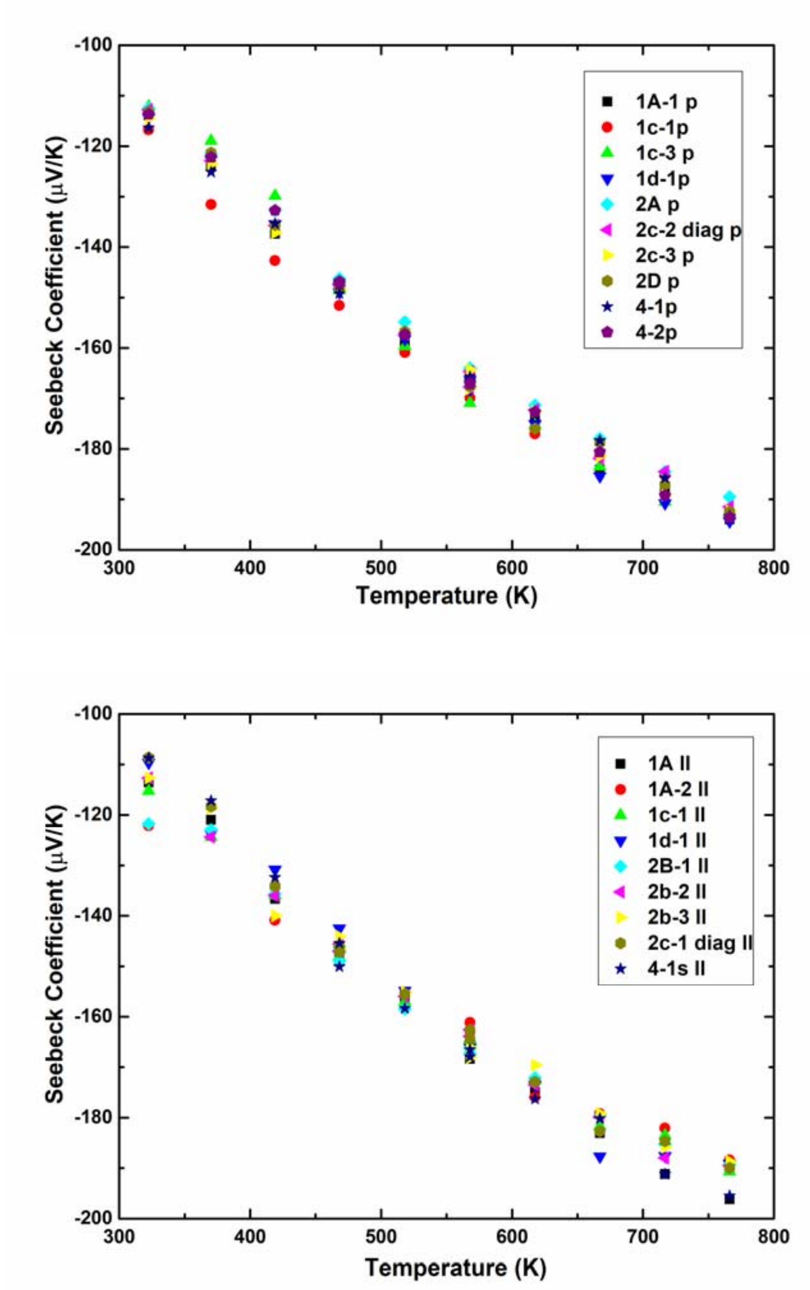

Figure S7. Seebeck coefficient vs temperature measurements on machined samples obtained as shown in Figure S3.

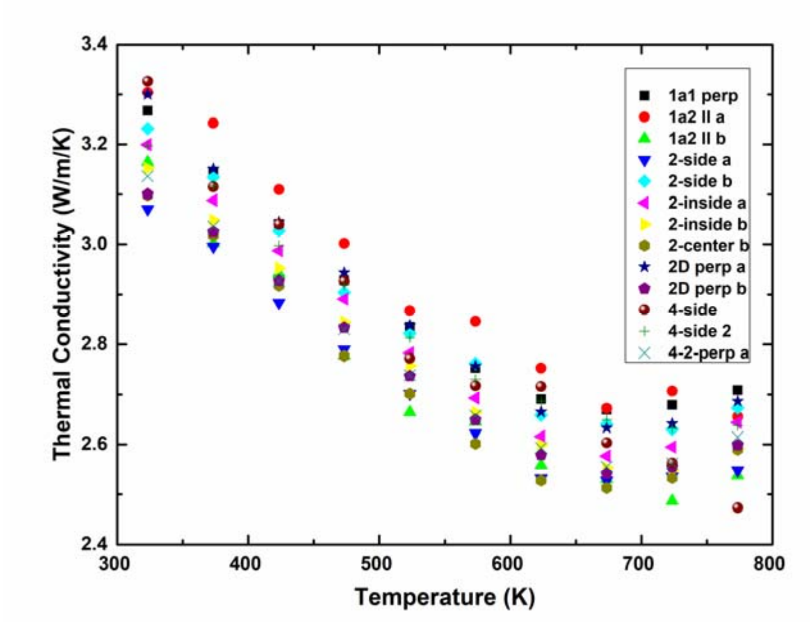

Figure S8. Thermal conductivity versus temperature measurements for samples machined from large pressed piece; samples are named according to their position and orientation within the large pressed piece.

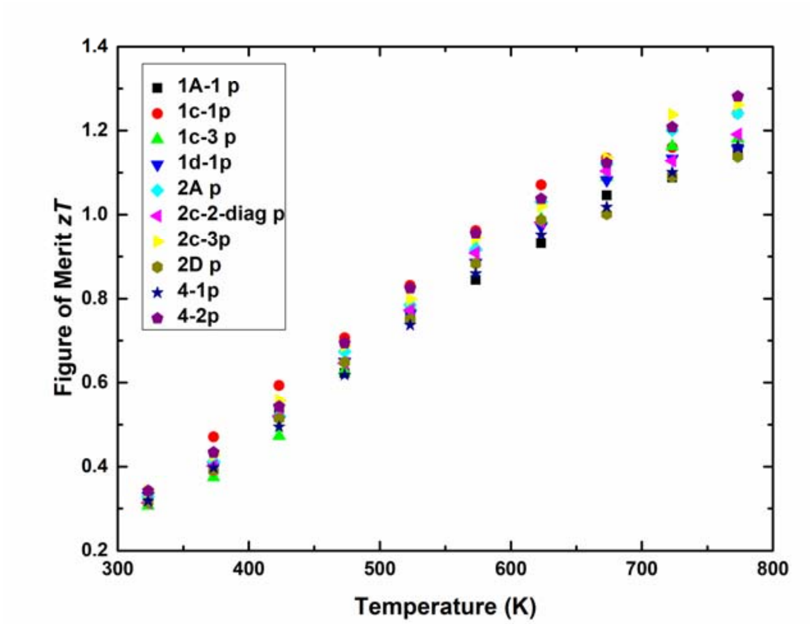

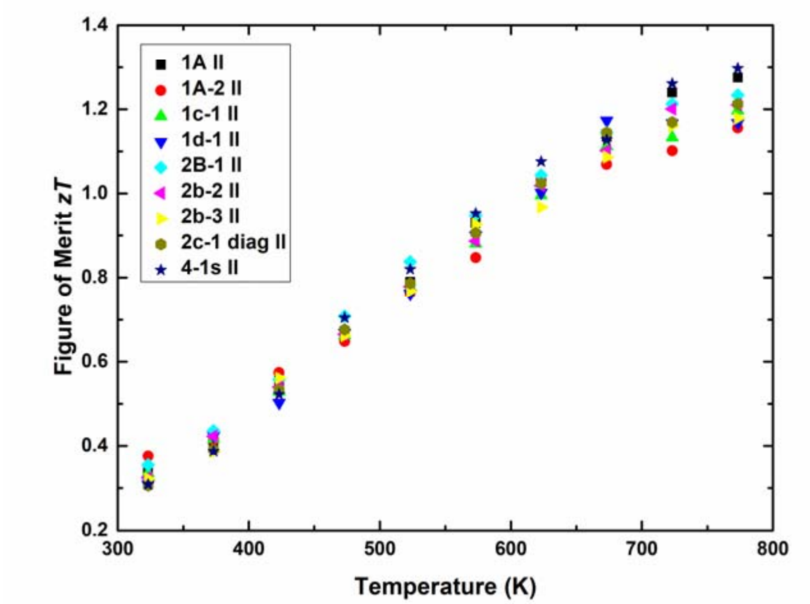

Figure S9. Perpendicular (top) and parallel (bottom) figure of merit versus temperature calculated using values obtained from electrical conductivity and Seebeck coefficient and average thermal conductivity values.

Table S1. Dimensions and densities for samples cut parallel to pressing direction used to measure electrical conductivity and Seebeck coefficient versus temperature.

Sample	Mass (g)	Depth (mm)	Width (mm)	Length (mm)	Density (g cm^{-3})
1a p	0.249	2.91	3.17	8.60	3.14
1a-1 p	0.198	3.15	2.30	8.64	3.16
1c-1p	0.151	2.29	2.34	8.86	3.18
1c-3p	0.143	2.35	2.14	9.02	3.15
1d-1 p	0.142	2.35	2.19	8.91	3.10
2a p	0.091	1.78	1.83	8.88	3.15
2c-2-diag p	0.149	2.33	2.31	8.73	3.17
2c-3p	0.137	2.32	2.12	8.63	3.23
2d p	0.137	2.10	2.29	8.94	3.19
4-1 p	0.145	2.22	2.35	8.83	3.15
4-2 p	0.143	2.29	2.23	8.90	3.15

Table S2. Dimensions and densities for samples cut perpendicular to pressing direction used to measure electrical conductivity and Seebeck coefficient versus temperature.

Sample	Mass (g)	Depth (mm)	Width (mm)	Length (mm)	Density (g cm^{-3})
1A ll	0.170	1.82	2.86	10.32	3.16
1a-2 ll	0.312	2.28	2.19	19.74	3.17
1c-1 ll	0.221	2.36	2.25	13.02	3.20
1d-1 ll	0.353	2.18	2.36	21.73	3.16
2b-1 ll	0.126	2.09	1.82	10.65	3.11
2b-2 ll	0.123	2.08	1.82	10.50	3.09
2b-3 ll	0.339	2.21	2.29	21.11	3.17
2c-1-diag ll	0.218	2.25	2.33	12.97	3.21
4-1s-ll	0.230	2.30	2.22	14.22	3.17

Table S3. Dimensions and densities for samples used to measure thermal diffusivity versus temperature.

Sample	Mass (g)	Depth (mm)	Width (mm)	Length (mm)	Density (g cm^{-3})
1-A-1-perp	3.08	8.69	9.98	0.838	3.14
1-A-2 ll a	0.69	8.89	8.82	0.149	2.75
1-A-2 ll b	0.79	9.85	8.15	0.190	3.00
2-side a	1.06	6.13	9.51	0.187	3.03
2-side b	1.17	9.08	6.47	0.217	3.16
2-inside a	1.76	7.80	9.21	0.396	3.13
2-inside b	1.78	9.17	9.83	0.503	3.13
2-center b	0.94	9.18	9.83	0.272	3.21
2D perp a	2.09	9.67	9.00	0.584	3.21
2D perp b	2.09	9.27	9.57	0.579	3.12
4 side	0.52	9.16	8.63	0.120	2.92
4 side 2	1.22	9.04	9.57	0.329	3.12
4-2-perp a	2.20	9.02	8.87	0.558	3.17